5-2019

High-Powered LED Assembly as Replacement for Conventional HBO Lamps in High Resolution, High Magnification Microscopy System

Christian Y. Miranda Solis
The University of Texas Rio Grande Valley

HIGH-POWERED LED ASSEMBLY AS REPLACEMENT FOR CONVENTIONAL HBO LAMPS IN HIGH RESOLUTION, HIGH MAGNIFICATION MICROSCOPY SYSTEM

A Thesis

by

CHRISTIAN Y. MIRANDA SOLIS

Submitted to the Graduate College of
The University of Texas Rio Grande Valley
In partial fulfillment of the requirements for the degree of

MASTER OF SCIENCE IN INTERDISCIPLINARY STUDIES

May 2019

Major Subject: Science and Technology

HIGH-POWERED LED ASSEMBLY AS REPLACEMENT FOR CONVENTIONAL HBO LAMPS IN HIGH RESOLUTION, HIGH MAGNIFICATION MICROSCOPY SYSTEM

A Thesis
by
CHRISTIAN Y. MIRANDA SOLIS

COMMITTEE MEMBERS

Dr. Natalia V. Guevara
Chair of Committee

Dr. Juan Guevara Jr.
Committee Member

Dr. Ahmed Touhami
Committee Member

Dr. Edgar Corpuz
Committee Member

May 2019

ABSTACT

Miranda Solis, Christian Y., High-Powered LED Assembly as Replacement for Conventional HBO Lamps in High Resolution, High Magnification Microscopy System. Master of Science (MS), May,2019, 39 pp., 15 figures, 1 table, 69 references.

Through decades, fluorescence microscopy has relied on mercury vapor lamps as its main light source due to their high power, broad spectrum, and bright bands generated. The use of mercury vapor lamps has remained fundamentally associated with the required lighting equipment of research laboratories. However, as time progresses, mercury vapor lamps have been slowly replaced with technologies that offered longer lifetimes, less hazardous waste, and output light at similar intensities. LED technology has been actively used in biological research, but were limited by price, lower intensities, and stability. Recent development of LED technology has allowed for further understanding and implementation in the fluorescence microscopy area. Thanks to the performance gains, newer high-power LEDs have proven to generate sufficient intensity to provide a useful light source for fluorescence microscopy. We developed a system capable of fully replacing conventional mercury-based lamps with high-power LED technology suited to yield specific spectra, and sufficient power output to produce quality results. Moreover, this system provides a cost effective, less hazardous alternative without the need of modifying conventional fluorescence microscopy systems

DEDICATION

The completion of my studies would not have been possible without the love, comprehension, and support of my family. My mother, Alma Solis, for your continuous support throughout my life, I would not be the man who I am today without you, and for that I will always be grateful to you. My brothers, Jesse Miranda Solis and Aldo Miranda Solis, for inspiring me to work for my dreams. My uncles, Jesus Solis Flores and Marco Solis Flores, for teaching me that the strength of a man comes from the support of their closest. My aunt, Patricia Solis, for showing me that love and resilience should never cease to exist in my heart and mind. My grandfather, Jesus Solis Huazo, for proving that mistakes are small compared to a good heart. My grandmother, Socorro Flores Mata, for the love, support, and teaching, but most important, for the family core she built. Last, but not least, I want to thank Alma Patricia Martinez for her unconditional support, for motivating me when I needed it, but most importantly, for helping me rise every time I fell. I will always be grateful for your love, care, and support. Thank you all.

ACKNOWLEDGMENTS

I want to thank Dr. Natalia Guevara, and Dr. Juan Guevara Jr., for all the mentoring and advice. You gave me confidence, and motivation to improve as a scientist, engineer, but most importantly, as a person. May all your lessons and advice guide me through my life and career. I will forever cherish the care, advice, and guidance.

I would also like to thank Dr. Ahmed Touhami for providing me my first experience as a scientist. I would not be here without the support you gave me to pursue science, even though it was outside your laboratory.

Moreover, I would like to thank Dr. Arlene Ready and Dr. Leslie Jones, for trusting me when I was not the safest option. My time at the Learning Center molded my entire academic life.

Thank you to every one of you.

Christian Yair Miranda Solis.

May 2019

TABLE OF CONTENTS

LIST OF FIGURES

Page

CHAPTER I

INTRODUCTION

The absorption and emission of light by specimens is the result of the physical phenomena of fluorescence or phosphorescence. Fluorescence is the emission of electromagnetic radiation caused by a chemical compound that when excited with a certain wavelength, irradiates light [1,2] Contrary to phosphorescence, fluorescence is directly dependent on the stimulant ray. In microscopy, fluorescence has become an essential tool due to the reduced constraints, the ability to observe definite molecular components through specific labeling, and the ability to obtain data of live samples in real time in comparison with other contrast techniques [4]. Subsequently, the application of fluorescing techniques has made possible to identify cell structure and sub-micron structures with high-level accuracy. Fluorescence microscopy has, most likely, been one of the major steps to determine cell structure. Thus, the understanding of once unresolved structures details the importance of fluorescence microscopy in modern scientific research [5,6,7]. However, conventional fluorescence microscopy is limited by several factors: the diffraction limit caused by the diffraction of light, and the need of powerful light sources to excite bio-marked molecules. The following establishes a background for the understanding of the development of improved fluorescence optical microscopy light sources that combine non-destructive techniques with a nano-scale resolution system capable of circumvolve diffraction laws to obtain improvements in contrast, lifetime, and fluorescence resolution of the samples.

1.1 The Diffraction Limit, and Rayleigh's Criterion

The resolution of optical imaging apparatus, microscopes, and telescopes was explained by the German physicist Ernst Abbe in 1873. In particular, Ernst Abbe elaborated in the dependence of the diffraction of light to the resolution achieved by optical instruments which would later be known as Abbe's theory [8,9]. According to Abbe's theory, images observed in the microscope are composed of an array of differing intensity spots stacked to produce an image [9,10]. Correspondingly, the best point source through an optical system is referred to as an Airy disk. Therefore, in order to understand the resolution of a microscope objective, the minimum resolvable distance, or Airy disk's radius of diffraction, is defined by the formula:

$$d = \frac{\lambda}{2n\ sin\theta} = \frac{\lambda}{2\ NA}$$

Where λ is the wavelength of light, and NA the numerical aperture of the objective lens [8,9,10]. Subsequently, Abbe's simplified equation was later refined by Lord Raleigh, in 1896, resulting in the Rayleigh's criterion. Rayleigh's criterion defines the shortest distance in which two fluorophores can be distinguished as separate objects, and is given by:

$$R = \frac{0.61\lambda}{NA}$$

In detail, Rayleigh's criterion is used to obtain the point spread function (PSF) related to the wavelength of light and the objective's aperture angle of a system. The width of the PSF regulates the previously mentioned distance of separation between two identical fluorophores where both can be resolved without merging into single point appearance [11]. Hence, in order to calculate the specific resolution of a system, the Rayleigh's criterion formula can be further adjusted to a higher degree that yields:

$$R = \frac{1.22\lambda}{NA(obj) + NA(cond)}$$

Where NA (obj) refers to the specific numerical aperture of the objective and NA (cond) to the numerical aperture of the condenser. This equation is to count for the behavior of the objective and condenser, however, an absolute value of these should never be considered [12].

1.2 Optical Microscopy

It is believed that the first compound microscope was built by Zacharias Jansen and, his father, Hans Lippershey in 1595 [13,14]. Jansen's microscope allowed magnification from 3 to 9 times the actual size of the sample with lenses encased in a two-tube system [15]. Subsequently, in the 17th century, Anton Van Leeuwenhoek, father of microbiology, created the microscopes with the greatest magnification of his time. The microscope was, arguably, capable of magnification up to 275 times. Significantly, Van Leeuwenhoek pioneered studies of protist, bacteria, cell vacuoles, spermatozoa, and capillary circulation [13,14,15]. Similarly, Robert Hooke, a contemporary of Van Leeuwenhoek, also made observations with a compound microscope. Hooke's apparatus was closer to what modern microscopes look, as it incorporated a stage for samples, light source, and three lenses. Despite being more complex, Hooke's microscope could not reach the quality of images obtained by Van Leeuwenhoek [14]. Nevertheless, it took until the nineteenth century to develop the blueprints of modern microscopy. Ernst Abbe, along with Otto Schott produced the first theory-based lenses that was able to produce diffraction-limited microscopes [8]. Beginning in 1872, Ernst Abbe and Carl Zeiss revised the microscope and started producing quality hardware with optics based on calculations made by Abbe that improved dramatically the magnification and resolution at that time. Moreover, Abbe invented the Abbe condenser, which allowed to focus light with multiple lenses but was quickly surpassed by August [16,17]. Kohler's illumination. Kohler Illumination is the predecessor to what we call "brightfield" and launched the predecessor of the UV

microscope. In consequence, several advances were made in line with a systematic scientific approach due to the successful collaboration between Abbe and Zeiss [18].

The scientific community had the desire to explore more biological samples but faced the challenge of their low contrast due to their refractive indexes being close to water. To begin with, this characteristic generated poor light scatter interaction with the incident light from the microscope [19,20]. Therefore, different methods like polarization changes, image phase, staining, and fluorescence have been developed ever since the invention of the microscope. Most biological samples generate contrast in common bright field apparatus by scattering and absorbing the incident light, but contrast is very poor [19,21]. In 1930, Fritz Zernike developed a method to generate contrast from phase rather than the amplitude of light by working with diffraction gratings. His observations, and later applications to the field of microscopy led him to be awarded the Nobel prize in 1953. Phase contrast is achieved by placing a circular annulus in front of the light source to produce a ring of light. The ring phase shifts the background light by 90˚, allowing the scattered light and the ring-shaped in phase to produce an increased contrast image [22,23,24,25]. However, one main disadvantage occurs when working with a dark background as the specimen appears lighter or with a halo outlining [22, 25]. A different method for unstained samples is differential interference contrast (DIC) created by F. H. Smith and later developed by G. Nomarski in 1955 [14 ,27]. Similarly to Phase contrast, DIC makes use of the polarization of two beams at a 90˚ angle between each other [28,29]. Both beams are focused through the objective lens and recombined through a Nomarski-Wollaston prism, shifting the phase difference between base pairs, emerging at polarization of 135˚. Using a Nomarski-Wollaston prism allows the total surface of the condenser aperture to be applied for the illumination of the sample [28,29,30]. Therefore, the sample will appear bright against a dark

background without the haloing effect obtained in phase contrast [28,31]. The produced image is exceptionally sharp when working with thin samples, as thickness or debris resulting in undesired phase changes [32].

1.3 Fluorescence Microscopy

Fluorescence microscopy developed as an improvement to ultraviolet microscopy. August Kohler and Moritz von Rohr developed the first UV microscope at the beginning of the twentieth century. Their system made use of a cadmium arc and fused quartz lenses to generate ultraviolet radiation that would illuminate the sample and emit a higher contrast light [33, 34]. Although the system was limited, it became the pivotal point for the development of fluorescence microscopy. Subsequently, by 1911, Oskar Heimstaedt had developed an outright fluorescence microscope by using cuvettes to filter all, but the UV light generated by an arc lamp. Heimstaedt was able to image bacteria but noted that the illumination system along with the dark field condensers limited the application of his microscope [35]. During the following decades, Max Haitinger devised the term ‘fluorochrome’ from his technique of secondary fluorescence. In like manner, Haitinger developed a system involving the addition of a contrast fluorescent chemical to his sample, and a light source placed on the same side of the sample as the objective, enabling the excitation and emission light passes through the objective. Specifically, Haitinger’s configuration allowed a more adequate excitation of the sample, and imaging of opaque objects [36, 37]. Notably, these systems were furtherly improved in 1929 by Phillipe Elinger and August Hlirt when they designed the prototype of the epi-fluorescence microscope. In their early design, the excitation light passed through a series of filters to obtain the right wavelength before hitting the objective lens and trigger the emission of the sample. Ellinger and Hirt imaged kidney and liver tissue injected with fluorescein and trypaflavin [38,

39]. Ultimately, with the invention of dichroic mirrors in 1967, their design would become the standard for fluorescent microscopes [33, 40].

1.4 Light sources: The Mercury Vapor Lamp

The mercury vapor lamp has been the central light source for fluorescent microscopy, since the beginning of the twentieth century, due to the bright bands it generates along the visible wavelengths. Correspondingly, when paired with appropriate filters, selected wavelengths could be achieved [41]. Thus, the mercury vapor lamp became highly reliable for scientific purposes. The most common mercury vapor lamp used is a 100-watt high-pressure mercury plasma arc-discharge lamp due to its highest radiance and luminance along with its small source size compared to any other lamp. Generally, the commercial name adopted is HBO lamps; H referring to, mercury, Hg, B is the symbol for luminance, and O for unforced cooling (HBO 100 for the 100-watt lamp) [41, 42, 43]. The benefits that the HBO lamps represented when compared to traditional incandescent lamps, were accompanied with several inconveniences like the mechanical alignment required, shorter lifetime, decrease homogeneity with time, and specialized housings along power supplies for its use. Moreover, over two-thirds of its output are in the ultraviolet and infrared spectrum. Therefore, care must be taken to protect the eyes and samples. The general lifetime of an HBO lamp is 200 hours, but it is dependent on how they are used. Generally, the 200-hour limit is compromised by the number of ignitions; as they should not exceed half of the rated hours at an average of 2 hours by ignition. By the nature of its use, just as the HBO lamps age, they blacken, making the ignition increasingly difficult. Regardless of its drawbacks, HBO lamps remain as the main illumination source for fluorescence microscopy, and one of the best illumination systems available [44].

1.5 Light Sources: LED Lighting

Light-emitting diodes were developed as a result of the study of Electroluminescence in 1907 by H.J. Round. Round realized that after a low potential was applied to a crystal of carborundum, the crystal would emit bright light. It was noted that the intensity varied according to the placement of the anode and cathode in the crystal along with the voltage applied [45]. Nevertheless, it was until 1927 when Oleg Losev, a Russian inventor, suggested the development of a system capable of irradiating constant luminescence after a carborundum crystal was subjected to a potential [46]. The phenomena kept being studied at a slow pace, in 1937 Georges Destriau reported electroluminescence with zinc sulfide, in the 1950's Kurt Lehovec, Accardo and Jamgochian elaborated with an apparatus using Silicon carbide crystals, but it was until 1963 that Texas instruments announced the first commercial LED with the SNX-110 [47, 48, 49]. The first attempt of commercialization of LEDs was in small devices due to their high cost of production. In 1970, Dr. Jean Hoerni, at Fairchild Semiconductor International, Inc., developed a process to fabricate LED devices for less than five cents [50]. Nevertheless, early diodes suffered from poor thermal management properties; applying any voltage to a small surface area caused overheating issues hence big heat sinks were needed to maintain appropriate working temperatures. Moreover, the power of the light emitted was significantly lower compared to traditional lighting systems. As a result, the applications to the scientific world were not the most efficient to replace conventional lightning methods [51, 52, 53, 54, 55].

Nowadays, LED technology has reached a peak. High powered diodes have been developed. These new diodes are capable of reaching the wavelengths of traditional systems and up to 140 lm/W [56]. In present times, the advantages of LED systems are noticeable. For example: LED efficiency is not affected by shape or size, producing more lumens per watt than

regular bulbs, Lifetime has been rated up from 10,000 to 25,000 hours with a warm-up time of less than a microsecond, and their comparatively low heat and IR radiation reducing the risk of sample damage [57, 51, 52, 53, 54, 55]. Nevertheless, disadvantages present include color rendition causing the color of objects to be perceived differently than actual, thermal runaway due to their low ambient temperature dependency, and high cost when high power is needed [51, 52, 53, 54, 55]. Despite the drawbacks, Fluorescence microscopy is one of the scientific fields that can benefit from the application of LED technology. The development of High-power systems capable of matching excitation wavelengths of fluorescent dyes and proteins can lead to a significant improvement of sample studies, and results [39, 58,59].

1.6 Fluorescence

The first reported observation of fluorescence was made in 1565 by a Spanish physician named Nicolas Monardes from an infusion of water and the wood of a Mexican tree. Monardes described the bluish opalescence of the infusion. The wood, later named *Lignum Nephriticum*, was studied by Boyle, Frampton, Newton, and others, but all failed to understand the phenomena [60, 61, 62]. In 1845, John Herschel, astronomer, studied *Lignum Nephriticum* and quinine sulfate solutions where he considered that the blue color of the solutions was a case of superficial color. Nevertheless, Herschel failed to consider that the solutions were too concentrated, causing the majority of the incident light to be absorbed, hence the blue color appeared to be solely superficial. Herschel's spectral analysis revealed blue, green, and some yellow with the use of a prism, but looked over the difference in length of the wavelengths between the superficial light(longer) and the incident light [60, 63,64]. The phenomena were later picked for study by Sir George Gabriel Stokes, where he demonstrated that the phenomena were a consequence of

the absorption of light. The term fluorescence was, first, introduced by Stokes in the middle of the nineteenth century [60, 65]

Fluorescence is an emission of electromagnetic radiation photons from an excited molecule, without a change in multiplicity [1 ,66]. The process involved in the excitation of a molecule can be visualized in the Perrin-Jablonski diagram (Fig. 1). In regular conditions, most molecules are in their lowest state S_0, shortly after absorption of a photon, their vibrational level can change to S_1 and fluoresce. Photon emission of a molecule is a nanosecond process and remain in their excited S_1 state before emitting a photon or undergo their de-excitation processes. The time a molecule remains fluorescing, or in its excited state S_1, before returning to ground state is called *excited state life*. The fluorescence intensity decay can be compared to other exponential processes like radioactive decay, which has a characteristic time called radioactive period that refers to the average lifetime of a radioactive element before degradation.

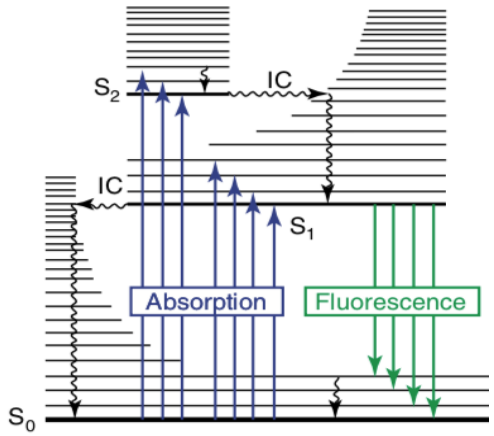

Figure 1 - Perrin-Jablonski Diagram. Fundamental electronic state are denoted S_0, Singlet states as S_1 and S_2. Diagram was modified from Valeur, Copyright Wiley-VCH Verlag GmbH & Co. KGaA.

In fluorescence microscopy, the process of fluorescence involves the absorption of energy (light) by an indicator in the molecule followed by the emission of light as a different

photon. Light towards the blue has a short wavelength, but higher energy than light towards the red with a longer wavelength [1, 66, 67] . In addition, due to the energy loss in the (this) excited state by vibrational relaxation, the fluorescence spectrum is located at a higher wavelength, lower energy, than the absorption spectrum. This gap between the maximum of the first absorption and the maximum of fluorescence is called Stokes shift. Usually, the gaps between the vibrational levels resemble each other in the ground state and excited state, thus the fluorescence spectrum is similar to the first absorption band, and this is known as the "mirror image" rule.

1.7 Stokes Shift

The Stokes shift is defined as the difference, in wavenumbers, between the first band in the absorption spectrum versus the first band of the emission spectrum:

$$\Delta\bar{\nu} = \overline{\nu_a} - \overline{\nu_f}$$

The difference varies according to the structure of the molecule and on the environment in which is tested.

According to the structure of the molecule, and the environment in which is tested, the Stokes shift will vary [66]. In microscopy, the detection of fluorescence is proportional to the length of the Stokes Shift.

CHAPTER II

METHODS

2.1 Zeiss Axiovert 25 CFL Inverted Microscope

The microscope used for the analysis of samples is a Zeiss Axiovert 25 CFL. The microscope is equipped with an adjustable binocular tube with a 10x magnification. The microscope is adapted with five high-grade objectives: Zeiss CP- Achromat 5x/0.12 ∞/-, Zeiss Plan-NeoFLUAR 10x/0.30 ∞/0.17, Zeiss LD A-Plan 20x/0.30 Ph1 ∞/1.0, Zeiss LD A-Plan 40x/0.50 Ph2 ∞/1.0, and a Zeiss LD Plan-NeoFLUAR 63x/0.75 Ph2 Korr ∞/0-1.5. A PRIOR Optiscan II computer-controlled stage is mounted to the body of the microscope, allowing displacement for exact positioning along the XYZ axis. The light sources of the system consist of an adjustable halogen light source with a variable voltage between 1.5 to 6 V with a 0.4 max aperture condenser at the top. Moreover, the microscope allows coupling with an HBO 50, mercury vapor lamp, for reflected light fluorescence. Standard phase contrast filters are used at the top, and mirror reflectors for the HBO lamp. The microscope permits documentation of the samples through a 35 mm camera mount.

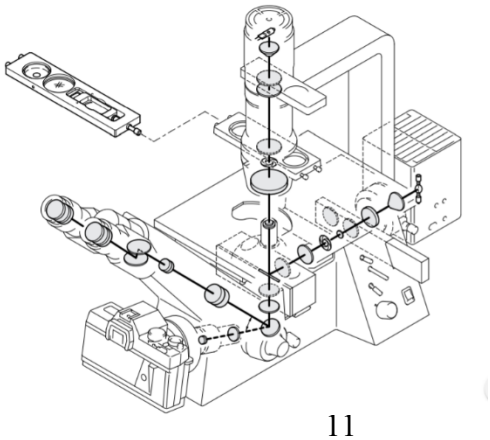

Figure 2- Optical Design of Axiovert 25 CFL which provides the schematics and location of the lenses and components of the system.

The Axiovert 25 CFL allows the coupling of an HBO 50 illuminator for reflected light fluorescence excitation of the sample. The power supply unit required for HBO 50 is a 220/240 V, 50- 60 Hz, 350 VA. The HBO 50 setup requires a Step-down transformer to be connected between the power supply unit and the HBO lamp housing. The HBO 50 lamp housing couples with the Axiovert 25 CFL through the designated backport.

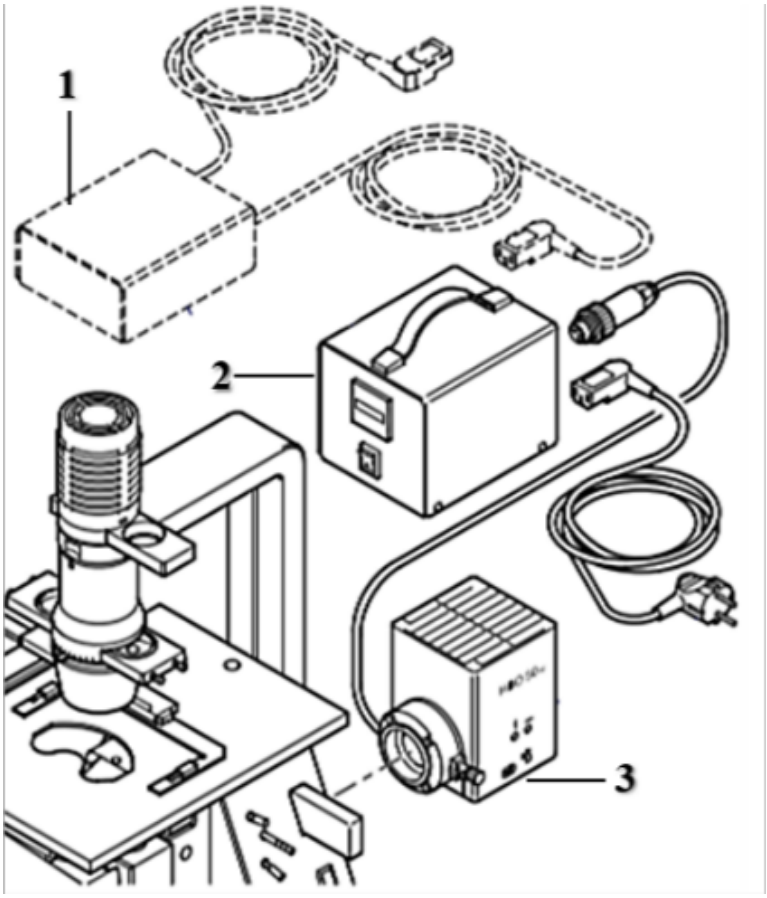

Figure 3 - Schematic of the HBO 50 Mercury Vapor Lamp. (1) Step-down transformer, (2) Power supply unit, (3) HBO 50 lamp housing.

2.3 LED Fluorescence Lamp- Version 1

The HBO 50 lamp housing assembly is constituted of three main components: the housing, the lamp mount, the mercury vapor lamp, and the aspherical collector. The mercury vapor lamp is held together by springs placed on the lamp mount. The aspherical collector is, also, held together by a system of springs accessible from the backside of the lamp mount. The lamp mount, in addition of the system to securing springs, encloses the series of adjusting screws for the light output. The assembly is tightened together by SW 30 screws accessible from the outer section of the lamp housing.

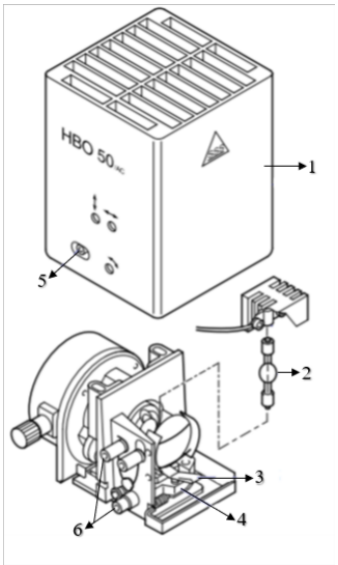

Figure 4- Internal schematic of the HBO 50 lamp housing. (1) External housing, (2) Mercury vapor lamp, (3) Spherical collector mount, (4) Mercury vapor lamp securing springs, (5) SW 30 securing screw hole, (6) Light adjusting screws.

The HBO 50 apparatus was modified to substitute the regular mercury bulb for a low energy 1.5 W dimmable G4 LED bulb. The internal electrical harness was modified to suit the G4 LED bulb. The transformer needed to power the system was eliminated, and the power supply replaced for a High-Voltage EC 105 power supply manufactured by E-C Apparatus Corporation. The EC 105 power supply allows the regulation of the light emitted from the LED

bulb. The knobs and adjustable points from the original apparatus were also modified to ensure that the adjustment of the collector, light output, and mounting point remained fully functional. The apparatus was powered with a high-voltage power supply set at 12V.

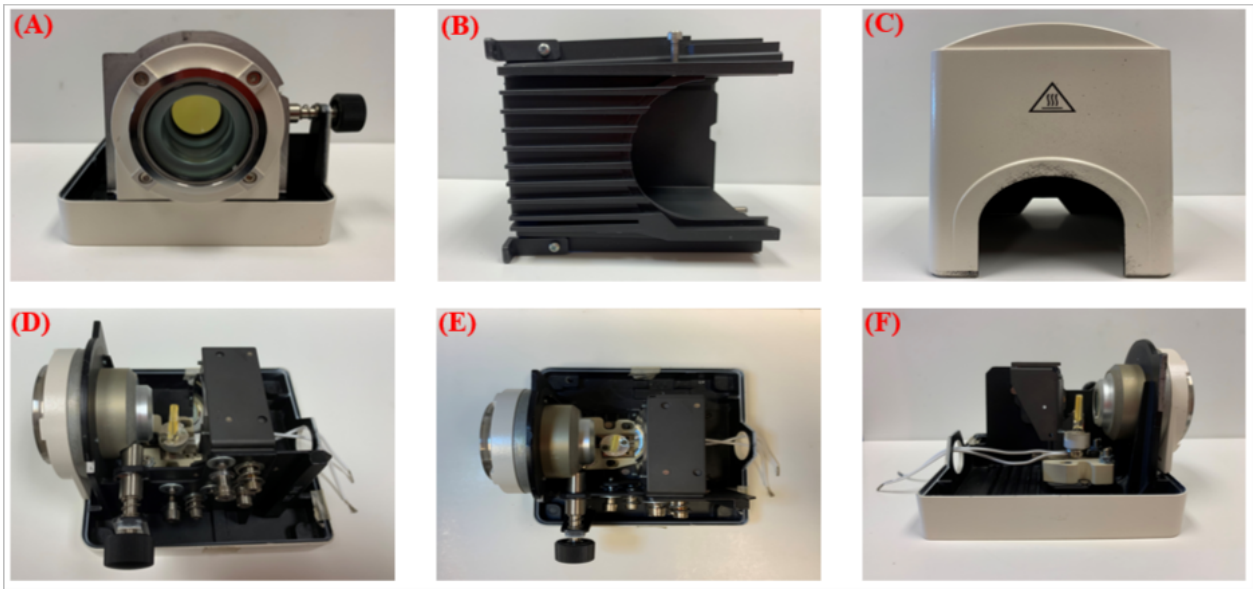

Figure 5 - Images of the modified HBO 50. (A) Front view of lamp mount. (B) Heat diffuser. (C) HBO 50 Lamp cover. (D, E, F) Modified Lamp Mount with functional adjustment knobs and LED bulb mount.

2.4 LED Fluorescence Lamp- Version 2

Version 1 of the LED-powered fluorescence lamp was further modified to fit a Thor Labs 6500K, 800mw, High Power LED. The High-Power LED, model number MCWHL5, outputs light at ≈ 450 nm, cold white, and has an estimated life of 10,000 h according to the manufacturer.

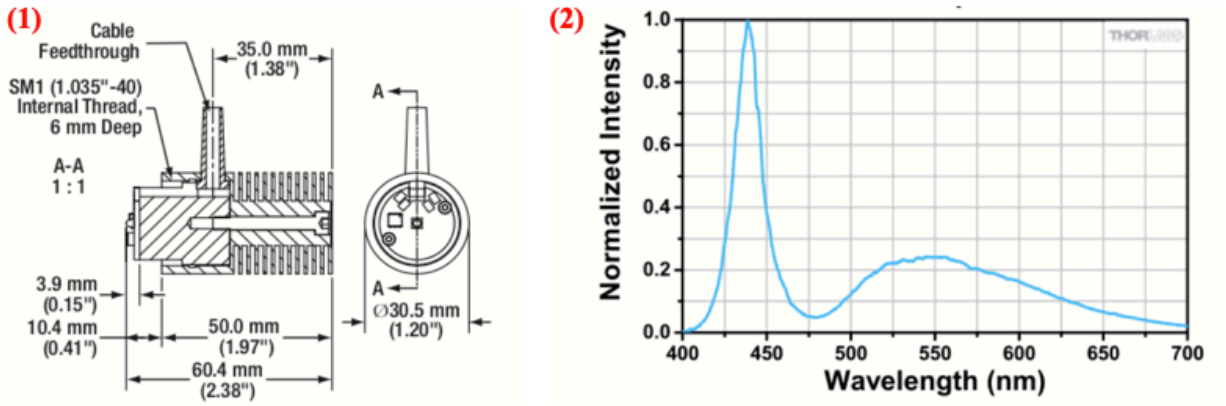

Figure 6 - Physical and Performance Characteristics of Thor Labs MCWHL5 High-Power LED. (1) Dimensional schematic of diode, (2) Output light spectrum. (Data obtained from Thor Labs, 25140-S01, Rev B, 2015)

In order to fit the High-Powered LED and retain the functionality of the adjustment knobs, the spherical collector was removed (Figure 3). The mounting brackets of the spherical collector were adapted to fit the housing of the High-Powered LED and secured back into its original place. The relatively small dimensions of the diode allowed proper fitment and placement in the mounting bracket. Furthermore, an aluminum ring was placed between the front part of the LED and the lenses of the original base in order to condense the maximum amount of light towards the lens (Figure 6, Image (4) through (6)). Plastic screws were used to secure both sections and allow the lens adjusting knob to remain functional. The dimensions of the complete assembly allowed the heat diffuser to be mounted in its original position and prevent any light leaks of the apparatus. Similarly, the external housing cover was reassembled without modification (Figure 6, Image (7) through (9)).

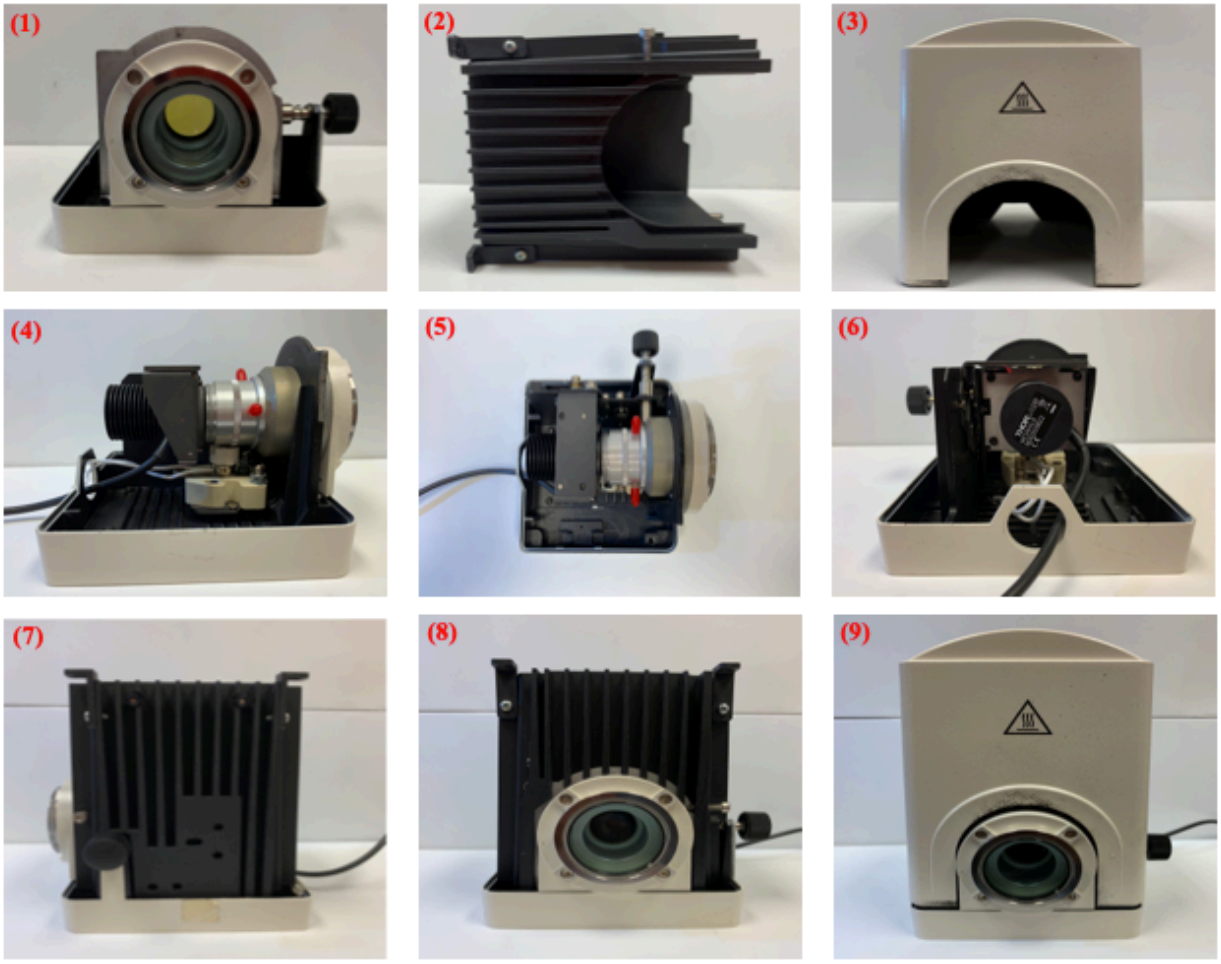

Figure 7- Version 2 LED fluorescence Lamp.(1) Front view of lamp mount, (2) Heat diffuser, (3) Lamp cover, (4) to (6) Side, Top, and back view of Version 2 LED fluorescence lamp with the High-Powered LED mounted, (7) and (8) show the heat diffuser secured with

Version 2 of the LED fluorescence Lamp is controlled by a unit developed by Alberto Villano for the Biophysics Research Lab in 2015 (Figure 8). The unit consists of a potentiometer that allows control of the input voltage to the High-Powered LED enabling different light intensity outputs, an output port to connect the LED, and a cutoff switch (Figure 8, Image (2)). The control unit is powered by a 24V, 2.5A AC Power Adapter.

As with Version 1, Version 2 mounts into the same position of the original HBO Mercury Vapor Lamp without further modification to the body of the microscope.

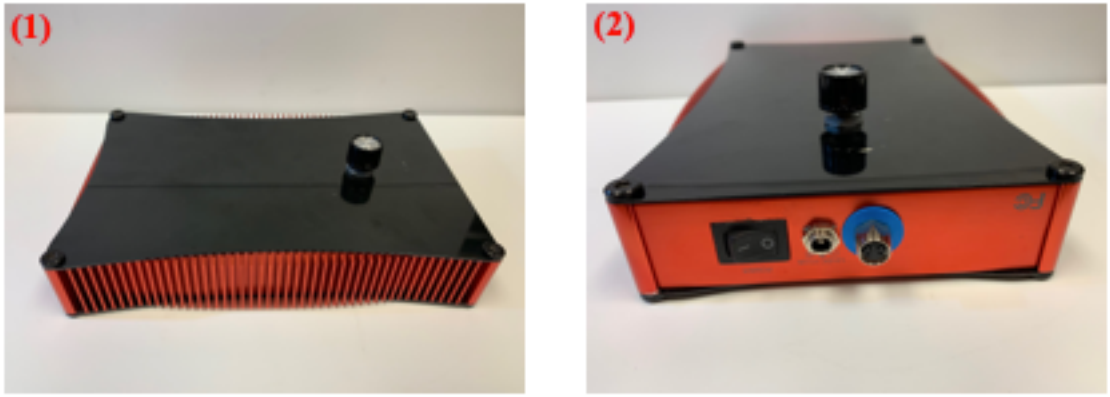

Figure 8 - Control Unit for Thor labs MCWHL5 High-Power LED developed by Alberto Villano. (1) Top view of control unit, at the top the potentiometer knob to control light intensity is located, (2) Sideview of the control unit where the switch and power outlets are located

2.5 Optronics CCD Camera

Optronics Microfire charged-coupled device camera was used to capture images due to its ability to capture fluorescence (Figure 9, Image (1), (3)). The original C-mount, 0.5x, was coupled for the purpose (Figure 9, Image (2)). The sensor contained in the camera is able to capture pictures up to 1600x1200 pixels. The field of view ranges from ≈ 4479µm at 5x to ≈363µm [69]. The camera is controlled through the PictureFrame software, where the contrast, gain, light, aperture time, among other settings can be controlled. Previously built modified C-Mounts were tried, but none allowed the camera to capture fluorescence. Figure 9, Image (4) shows the Optronics camera coupled with the original C-mount.

Figure 9 - Optronics Microfire camera. (1) Front view, (2) 0.5x C-Mount attatchment, (3) Back view, (4) Optronics Microfire camera coupled with 0.5x C-Mount.

2.6 Dino-Lite Digital Microscope Camera

Four different digital microscope cameras (DMCs) were tested to capture fluorescence. The devices were purchased from AnMO electronics corporation Dino-Lite Digital Microscope's website. Accordingly, the DMCs' specifications were obtained from the manufacturer. The first DMC (Figure 10, Image (1)) from the "Premier series", model number AM7013MZT is equipped with a 5-megapixel sensor, and maximum magnification of 200x at a resolution of 2592x1944. Similarly, the second camera, model number AM4113TS from the "Premier series", incorporates a 1.3-megapixel sensor capable of a maximum magnification of 220x.Thirdly, the next DMC (Figure 10, Image (3)) from the "Edge Series", model number AM7515MT89, incorporates a 5-megapixel sensor capable of resolution up to 2592x1944 pixels, magnification of 700x up to 900x with automatic magnification readings. The fourth DMC (Figure 10, Image (4)) from the "Edge series", model number AM4515T8, has a light sensor of 1.3-megapixels,

and a similar maximum magnification as the previous [68]. The cameras are controlled through Dino-Lite developed software and are powered through a USB port in the computer. It is important to note that the manufacturer does not specify that the sensors in these models are capable of fluorescence sensitivity. The DMCs were chosen, for fluorescence sensitivity testing, as previous studies, performed by Jaime Romo Jr in "Optical Method for Imaging and Video Recording Live Cultured Hela Cells at High Resolution, High Magnification", have proven that when coupled whit the Zeiss Axiovert 25 CFL Inverted Microscope, the magnification of the system reaches between 5220.42x to 21608.64x[69]. Nevertheless, it was unclear if the system would retain this potential magnification with the power of the LED fluorescence lamp as main light source for fluorescence studies. In order to fit the Dino-Lite Digital Microscopes into the body of the microscope, an aluminum sleeve, manufactured by Mr. Antonio Suarez machine shop supervisor, along with a rubber O-ring were used (Figure 11).

Figure 10 - Dino-Lite Digital Microscope Cameras. (1) Dino-Lite Premier, model number AM7013MZT with a 5-megapixel sensor, and maximum magnification of 200x. (2) Dino-Lite Premier model number AM4113TS with a 1.3-megapixel sensor capable of a maximum magnification of 220x. ,(3) Dino-Lite Premier Edge, model number AM7515MT89 with a 5 megapixel sensor, magnification from 700x to 900x and max resolution of 2592x1944, (4) Dino-Lite Edge, model number AM4515T8.

Figure 11-– Set-up needed to fit a Dino-lite Digital Microscope Camera into the viewing port of the Axiovert 25 CFL Inverted microscope. (1) Aluminum sleeve developed by Mr. Antonio Suarez at the UTRGV machine shop for the Biophysics Research Lab, (2) Dino-Lite Premier, (3) Dino-Lite Digital Microscope Camera coupled with the aluminum sleeve and the rubber O-ring.

2.7 Microscope Configuration

As previously mentioned, the coupling of the DMCs with the Zeiss Axiovert 25 inverted microscope significantly increases the magnification, and resolution power of the system. Therefore, the main configuration used in this study was the coupling of a digital microscope camera inserted in the frontal cavity of the microscope body at a distance of 11.78 cm of the mirror to the DMC in order to test if a resolution between 23611.85 pix/ μm^2 and 5513.06 pix/ μm^2 could be maintained when replacing the mercury vapor lamp for the high power LED lamp in fluorescence studies.

2.8 Isolation of Low-Density Lipoproteins

Low-Density Lipoproteins, LDL, were isolated from human plasma by sequential ultracentrifugation in NaCl solutions yielding 1.35- 0.9 g/ml density range of LDL. After purification, LDL was dialyzed in PBS and 10 mM $MgCl_2$. LDL was then slow filtered using a 0.2 µm filter. The DNA binding capacity of the LDL preparation was demonstrated using, EMSA, electrophoretic mobility shift assay. After the DNA binding capacity of the LDL sample, it was stored at -18 C˚ until further use.

2.9 Purified DNA

DNA was purified *in situ* for this study by Natalia Guevara, PhD. The purity of the DNA was not relevant for this study as the qualitative result of the DNA when labeled with fluorescent nucleic acid stain was the main subject of interest.

2.10 Synthetic Peptide

Fluorescein (FITC) Dengue virus envelop protein peptide was slowly brought up to 37 C° from dropwise storage. The peptide was added at a 1:5 ratio for experimentation.

2.11 Dextran Sulfate Cellulose Beads

Dextran Sulfate Cellulose beads were purchased from Kaneka Americas Holding Inc. The beads were submerged in 1x PBS and 10 mM $MgCl_2$ and stored at -18 C˚ until needed. When experimenting, 8 µl of this stock solution were added to a mix with the FITC labeled peptide to test for fluorescence under the Axiovert 25 CFL LED HBO 50 set-up.

2.12 Escherichia Coli Cultures

Standard Escherichia coli (E.coli) cultures expressing red fluorescent protein (DsRed) were donated by Daniele Provenzano, PhD from the Biology Department at the University of Texas Rio Grande Valley. Cultures were maintained at 4 C° until ready for experimentation.

2.13 Image J Software

Image J, Image Processing and Analysis in Java, is an open source software for image processing and analysis with more than 1700 users and developers. Images obtained from Axiovert 25 CFL were processed through the software.

CHAPTER III

RESULTS

3.1 Light Leakage

One of the main concerns with the development of the LED fluorescence lamp for the Axiovert CFL microscope was light leakage of the system as it would represent a decrease in the light intensity from the system to the studied sample not allowing the camera sensors to pick up any data. Nevertheless, the perfect fitment among the components of the apparatus assured the maximum containment of the light emitted by the High-power LED. One of the principal constraints was the metal coupler used between the High-Power LED and the lenses of the mounting base of the HBO lamp, as there was no support from the bottom section of the base. For this purpose, the LED socket from V.1was reattached in the securing springs of the mercury vapor lamp, creating a convenient bottom support for the coupler. Consequently, the fitment among the lenses, coupler, and diode was considerably improved. The improved fitment allowed all of the focusing knobs to work perfectly, and the beam to be centered properly through the focusing lensed. This simple addition prevented any light leak from the apparatus regardless of the adjustments made to focus the beam of light.

In addition of the internal modifications, the original heat diffuser cover, and outside case were placed in their original coupling spots; allowing the system to contain light and dissipate heat when the system is functioning.

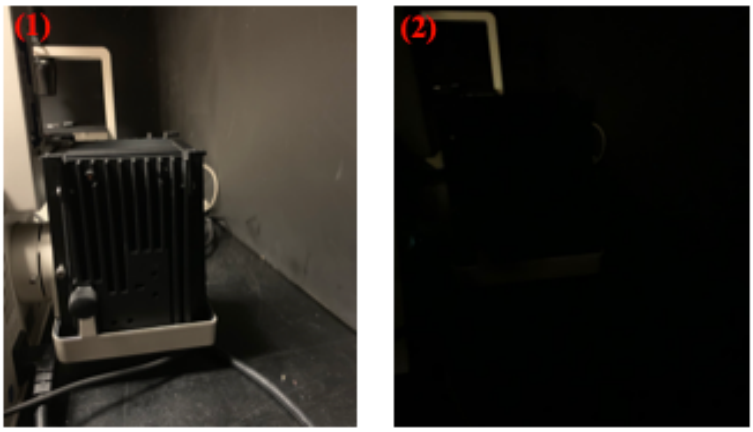

Figure 12 – Mounted LED Fluorescence Lamp. (1) Mounted LED Fluorescence Lamp into Zeiss Axiovert 25 CFL , (2) Running LED Fluorescence Lamp with lights off proves no light leakage from modified apparatus.

3.2 Micrometer Scale Control

It becomes necessary to establish the resolution of the images obtained in order to determine if the system retains its maximum resolution characteristics when detecting fluorescence when coupled with the LED fluorescence lamp. Therefore, the understanding of the potential fluorescence resolution will provide suitable parameters for the system and determining the studies in which the system is convenient to use. The collection of micrometer images shown in Figure 13 were obtained from the three different camera setups that were capable of capturing fluorescence: Optronics Microfire camera coupled with stock 0,5x C-mount, Dino-Lite Premier model number AM7013MZT, and Dino-Lite Premier model number AM4113TS. Contrary to the Optronics Microfire camera, the digital microscopes allow different magnifications. In order to find the best parameters to capture fluorescence, images were taken in four different magnification configurations of the DMCs: 100x (B1 to B5), 150x (C1 to C5), 200x (D1 to D5),

and 220x (E1 to E5). The maximum field of view in which the DMCs are capable of detecting fluorescence, ≈ 34.5µm, is reached at a total magnification of ≈ 5220.4x from the system[69]. The micrometer used has a scale of 100 µm divided into 2 µm sections. Images were enhanced by reducing noise, contrast, and adjusting color in Image J as mentioned in section 2.13. The different camera configurations captured images through the different magnification settings of the Zeiss Axiovert 25 CFL described in section 2.1.

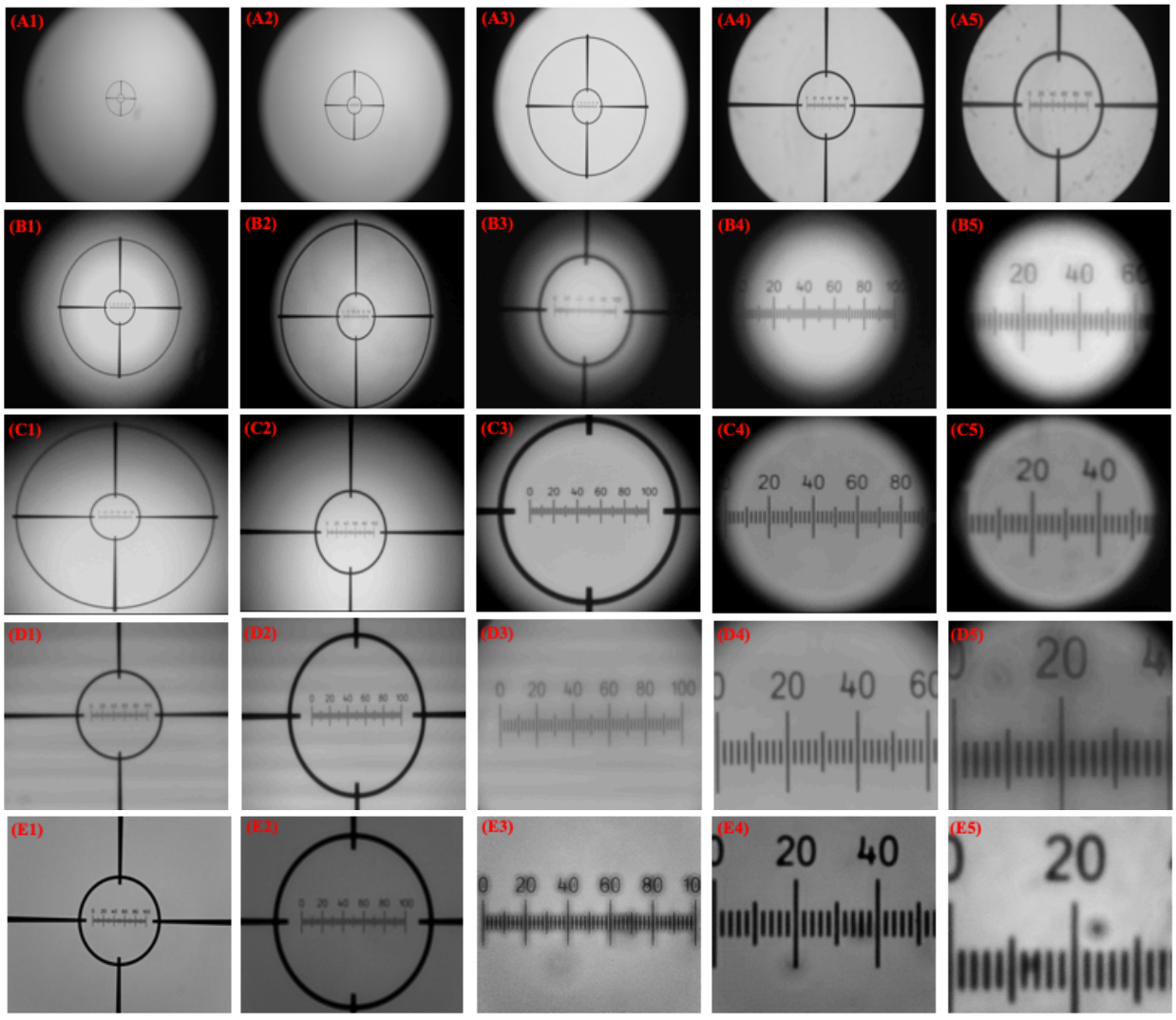

Figure 13- Images of Micrometer used for scaling. Zeiss Axiovert CFL microscope turret coupled with the following objectives: Zeiss CP- Achromat 5x/0.12 ∞/-, Zeiss Plan-NeoFLUAR 10x/0.30 ∞/0.17, Zeiss LD A-Plan 20x/0.30 Ph1 ∞/1.0, Zeiss LD A-Plan 40x/0.50 Ph2 ∞/1.0, and a Zeiss LD Plan-NeoFLUAR 63x/0.75 Ph2 Korr ∞/0-1.5 (A1) to (A5) Microfire Optronics CCD camera coupled with 0.5x C-mount through the objectives listed in section 3.2, (B1) to (B5) Dino-Lite Premier at 100x magnification, (C1) to (C5) Dino-Lite Premier at 150x magnification, and (d1) to (D5) Dino-Lite Premier at 200x magnification. The images captured with the Dino-Lite Premier camera were saved at 1280x1240 pixels

3.3 Dextran Sulfate Cellulose Beads

Resolving a biological sample that contains millions of fluorophores at a high resolution, high magnification can be a difficult task to resolve, as they are usually surrounded by a medium (PBS or DMEM) in a tray. In order to prove that the LED fluorescence lamp would be able to be produce sufficient power to excite the fluorescent molecules, a simple experiment attaching labeled peptide to DSC beads was performed. A solution prepared with 200µl of 10mM PBS/ $MgCl_2$, 5 µl of synthetic labeled peptide, and 8µl of DCS beads, was incubated for 30 minutes and placed in a µ-Slide 8 Well Glass Bottom to be examined under the microscope. The sample was then observed under bright light and a pair of DCS beads that showed clusters of the peptide attached to the surface was selected as a reference. The samples were, then, excited using the LED Fluorescence Lamp V.2 from section 2.4. The light beam wavelength was filtered to 470 nm using the filtering lenses in the Zeiss Axiovert 25 CFL. When observed from the ocular tubes, fluorescence was clearly observed, but concerns regarding the sensitivity of the sensors to capture fluorescence were present due to the non-fluorescence sensitivity described by the manufacturer of the digital microscopes. All of the cameras listed in Section 2.5 and 2.6 were tested. Only the Microfire Optronics (section 2.6) was able to capture fluorescence without further adjustment. Regarding the Dino-Lite Digital Microscope Cameras, only the Dino-Lite Premier, model number AM7013MZT, and model number AM4113TS were able to capture

fluorescence under certain magnification adjustments; not in every setting fluorescence was able to be captured with the same quality. Regardless of the quality, the images obtained in fluorescence can be further processed with Image J to obtain research grade quality. Figure 14 displays the images obtained, both in bright light and fluorescence with the Microfire Optronics CCD camera through the objectives listed in Section 2.1. The resolution of the pictures was set to 1600x1200, and no color correction or editing was done. Subsequently, Figure 15 were captured with Dino-Lite DMC Premier with a resolution of 1280x1240. The DMC settings were adjusted to 100x, 150x, 200x, and 220x. Again, no color corrections were made to the bright field images, but contrast and exposure were adjusted for fluorescence. Thirdly, Figure 16 images were captured using Dino-Lite DMC Premier AM4113TS with a resolution of 1280x1240. Similarly, the same adjustments to the previously mentioned DMC were used. Unlike DMC Premier AM7013MZT, the sensor, and lens set-up found in the DMC Premier AM4113TS proved to be more sensitive to capture fluorescence. Additionally, the images captured (Figure 16) displayed depth, and topography due to the intensity of the LED Fluorescence lamp.

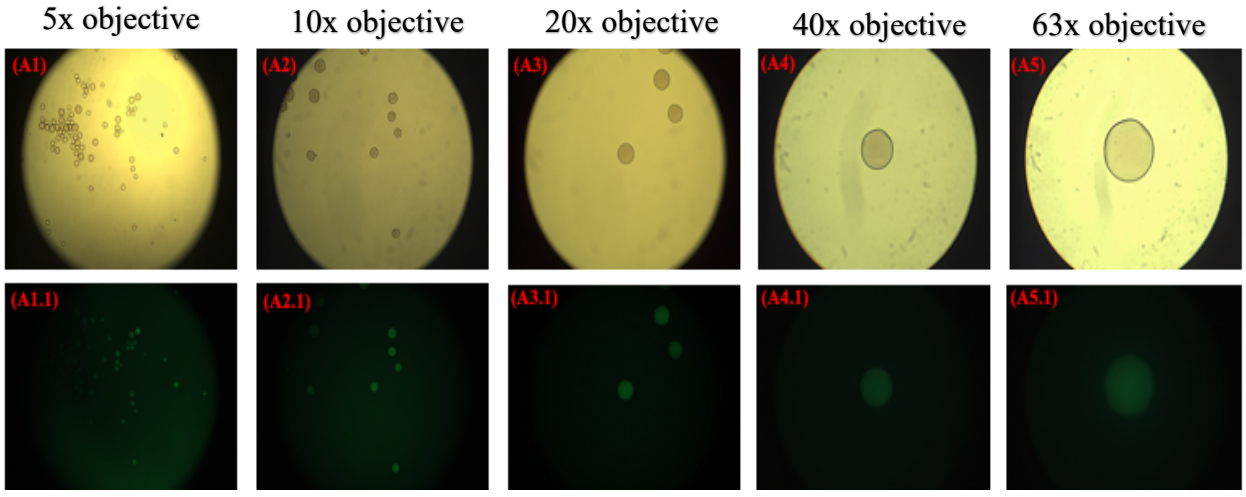

Figure 14 - (A1) to (A5) Images captured with Microfire Optronics coupled with 0.5x C-Mount and LED Fluorescence Lamp in Zeiss Axiovert 25 CFL at 1600x1200 pixels. The objective lens configuration in the Axiovert 25 CFL as follows: 5x (A1), 10x (A2), 20x (A3), 40x (A4), 63x (A5).

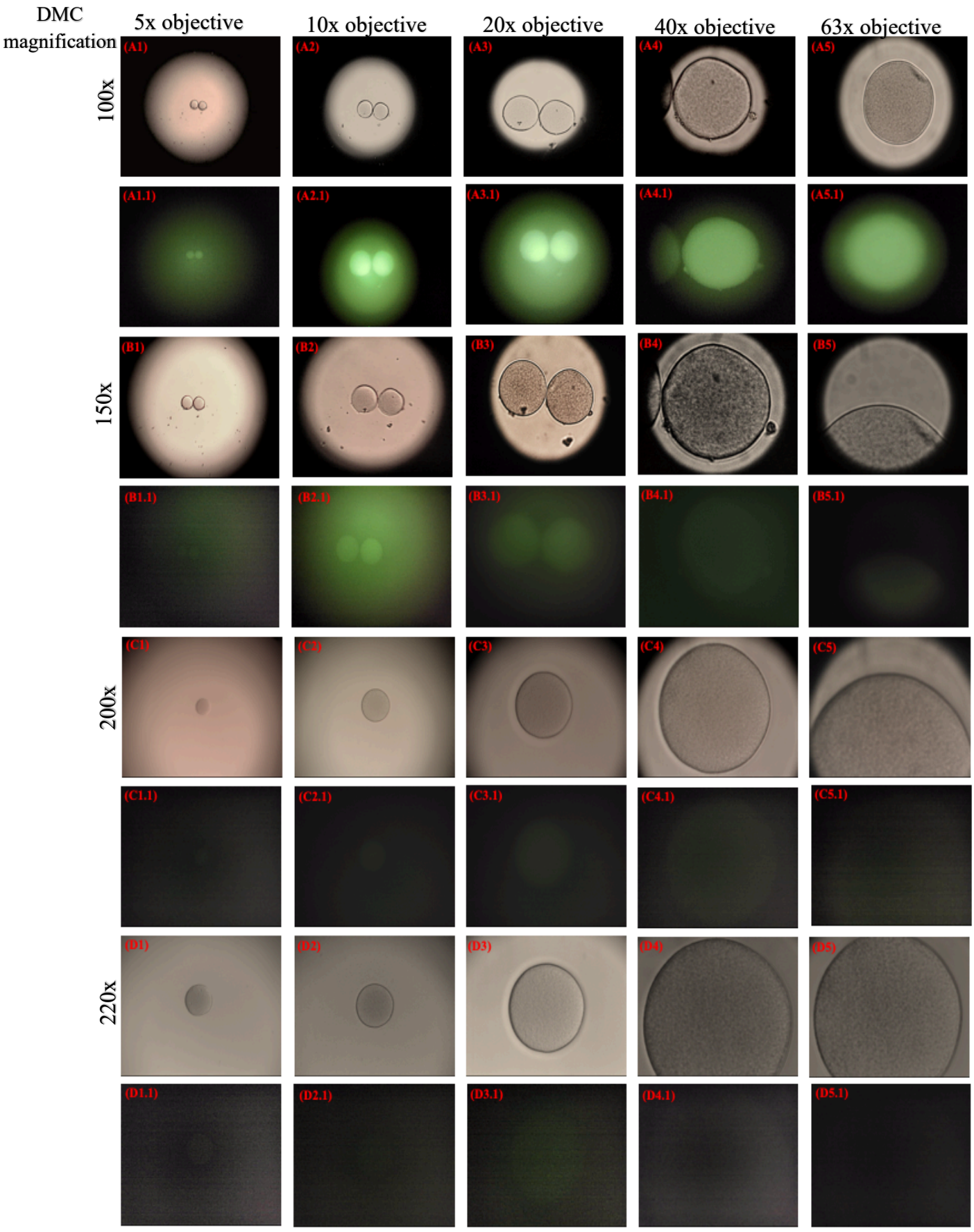
DMC magnification
5x objective
10x objective
20x objective
40x objective
63x objective
100x
150x
200x
220x
(A1)
(A2)
(A3)
(A4)
(A5)
(A1.1)
(A2.1)
(A3.1)
(A4.1)
(A5.1)
(B1)
(B2)
(B3)
(B4)
(B5)
(B1.1)
(B2.1)
(B3.1)
(B4.1)
(B5.1)
(C1)
(C2)
(C3)
(C4)
(C5)
(C1.1)
(C2.1)
(C3.1)
(C4.1)
(C5.1)
(D1)
(D2)
(D3)
(D4)
(D5)
(D1.1)
(D2.1)
(D3.1)
(D4.1)
(D5.1)

Figure 15 – Images captured with Dino-Lite Digital Microscope camera, model number AM7013MZT. Images *A1 to A5 captured with Dino-Lite DMC Premier, at 100x resolution, under bright light, A1.1 to B1.5 Images captured with Dino-Lite DMC Premier, at 100x magnification and LED Fluorescence Lamp V.2 in Zeiss Axiovert 25 CFL, (C1) to (C5) Images captured at 150x resolution, under bright light, (B1.1) to (B5.1) Images captured with Dino-Lite DMC Premier, at 150x resolution with LED Fluorescence Lamp V.2 in Zeiss Axiovert 25 CFL. (D1) to (D5) Images captured at 200x resolution, under bright light, (D1.1) to (D5.1) Images captured with Dino-Lite DMC Premier, at 150x resolution with LED Fluorescence Lamp V.2 in Zeiss Axiovert 25 CFL. (E1) to (E5) Images captured at 220x resolution, under bright light, (E1.1) to (E5.1) Images captured with Dino-Lite DMC Premier, at 220x resolution with LED Fluorescence Lamp V.2 in Zeiss Axiovert 25 CFL*

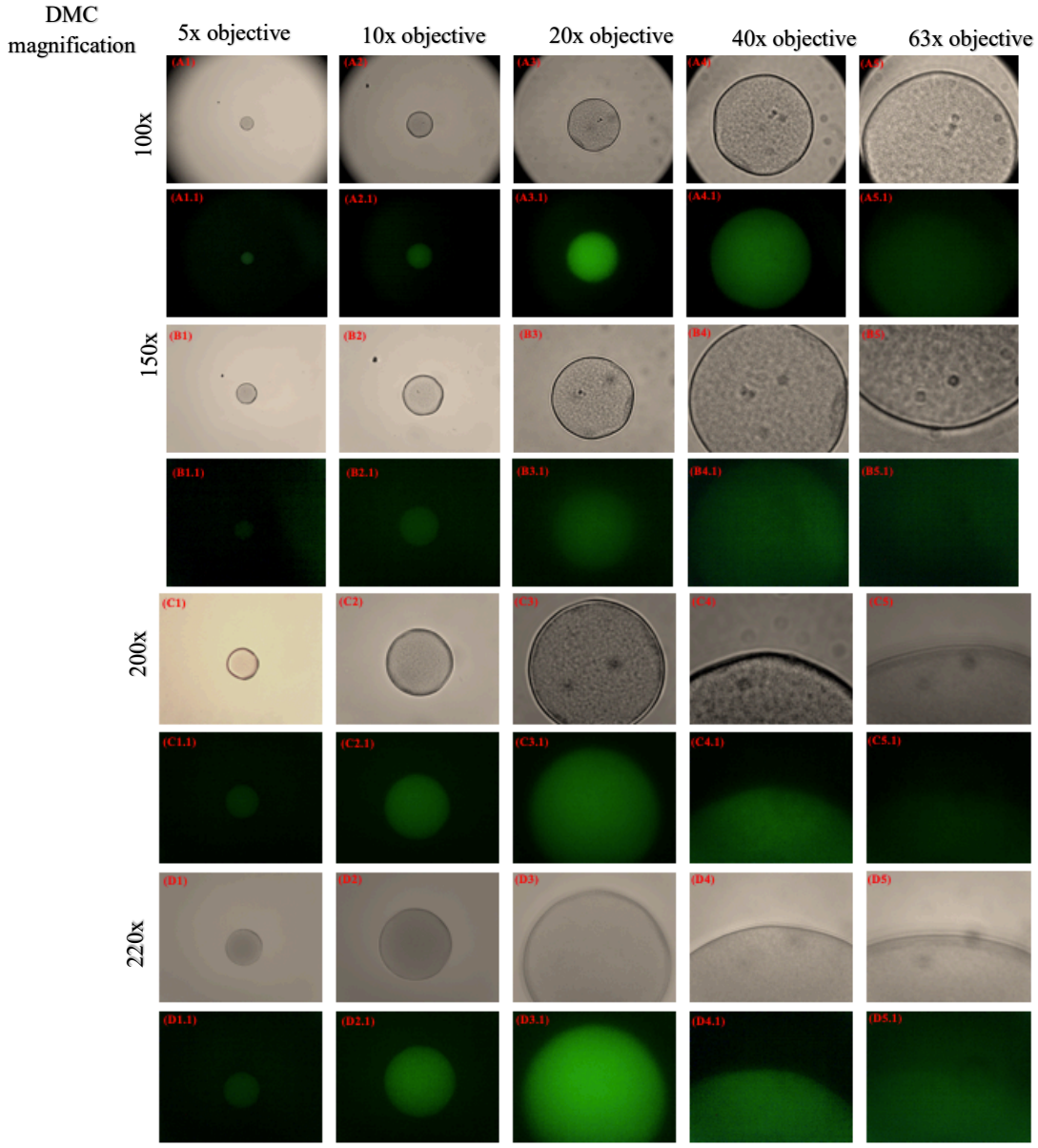

Figure 16- Images captured with Dino-Lite Digital Microscope camera, model number AM4113TS. Images A1 to A5 captured with Dino-Lite DMC Premier, at 100x resolution, under bright light, A1.1 to B1.5 Images captured with Dino-Lite DMC Premier, at 100x magnification and LED Fluorescence Lamp V.2 in Zeiss Axiovert 25 CFL, (C1) to (C5) Images captured at 150x resolution, under bright light, (B1.1) to (B5.1) Images captured with Dino-Lite DMC Premier, at 150x resolution with LED Fluorescence Lamp V.2 in Zeiss Axiovert 25 CFL. (D1) to (D5) Images captured at 200x resolution, under bright light, (D1.1) to (D5.1) Images captured with Dino-Lite DMC Premier, at 150x resolution with LED Fluorescence Lamp V.2 in Zeiss Axiovert 25 CFL. (E1) to (E5) Images captured at 220x resolution, under bright light, (E1.1) to (E5.1) Images captured with Dino-Lite DMC Premier, at 220x resolution with LED Fluorescence Lamp V.2 in Zeiss Axiovert 25 CFL

3.4 Labeled DNA with BOBO-1

Different labels needed to be tested in order to confirm the capacity of the LED Fluorescence Lamp to properly excite the fluorophores and allow the molecule to emit fluorescence. Purified DNA was labeled with a dilution of BOBO-1 in 10mM PBS/ $MgCl_2$, refer to Section 2.10 for dilution preparation, and placed in a cotton matrix for easier localization. Finally, the sample was then placed in a μ-Slide 8 Well Glass Bottom and placed under the microscope. The objective of placing the labeled DNA in the cotton fibers was to test the intensity of the LED fluorescence lamp when directed at a highly crowded sample. The samples were observed at first under bright light and then switched to fluorescence. Images were captured using the Optronics CCD Camera coupled with the 0.5 C-Mount at a 1600x1400 resolution. Figure 17 shows DNA clusters trapped in the cotton fibers through the different objectives listed in Section 2.1. The images captured under bright light show the shadows produced by the cotton fibers along with the DNA clusters making them hard to observe at a glance. On the other hand, when the condenser light is turned

off, and the LED fluorescence lamp is running, clearly visible labeled DNA clusters are excited and emit fluorescence.

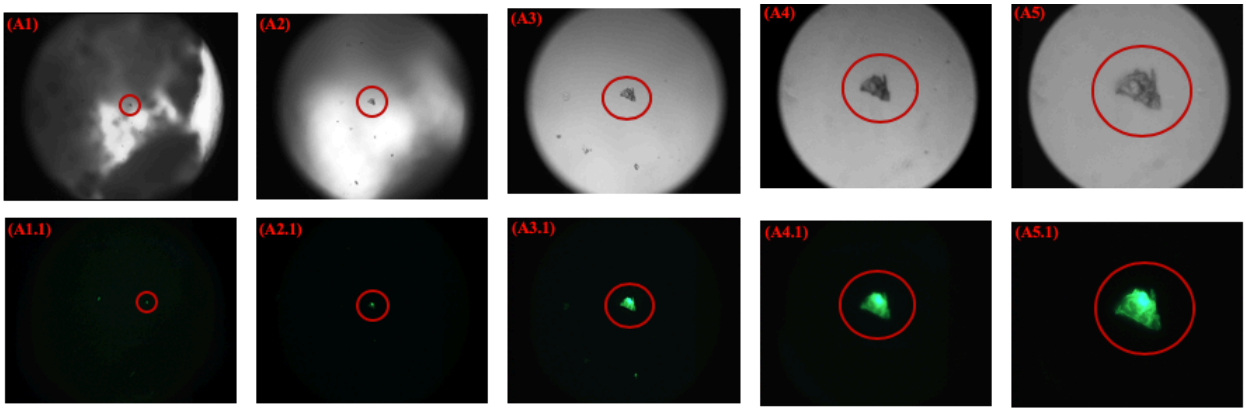

Figure 17 - Labeled DNA in cotton matrix. (A1) to (A5) images were captured with Microfire Optronics CCD camera coupled with 0.5C-Mount at 1600x1400 pixel resolution. Images were taken under bright light, (A1.1) to (A5.1) Images captures with Microfire Optronics CCD camera coupled with 0.5 C-Mount and LED Fluorescence Lamp in Zeiss Axiovert 25 CFL.

3.5 E.Coli Expressing DsRed fluoresncence Protein

In order to confirm the compatibility of the LED fluorescence lamp with the different excitation filters in the microscope, E.coli cells expressing Ds Red were observed with the Microfire Optronics camera and DMC Dino-Lite Premier AM4113TS. Detection of the emission was clear, and the size of the cell was able to be determined.

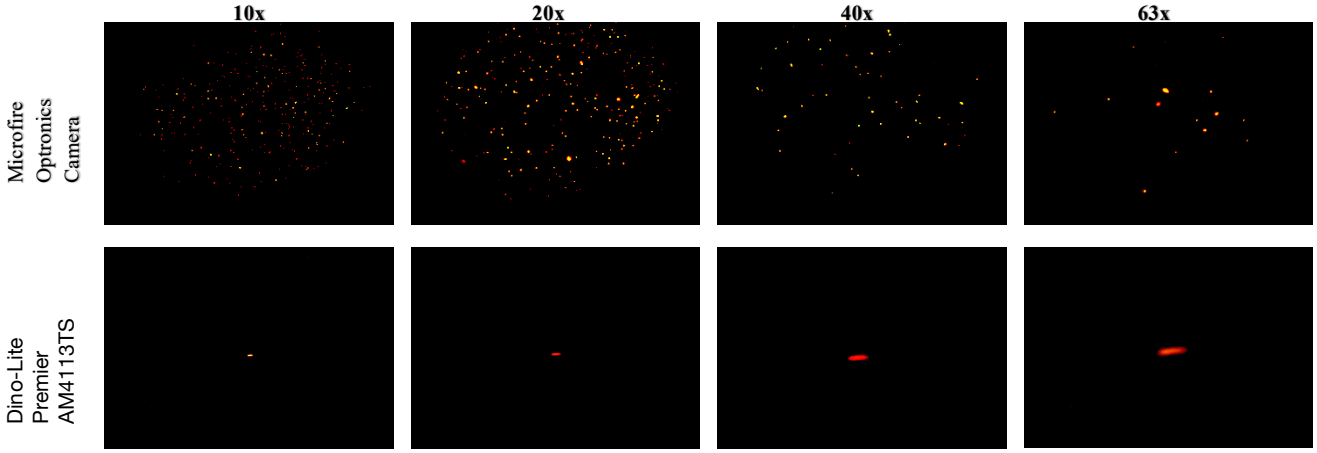

Figure 18 – Images of E.Coli expressing DsRed. Top row images were captured with Microfire Optronics CCD camera coupled with 0.5C-Mount at 1600x1400. Bottom images captured with Dino-Lite Digital Microscope camera, model number AM4113TS at 220x resolution with LED Fluorescence Lamp V.2 in Zeiss Axiovert 25 CFL

3.6 Physical Advantages of LED Fluorescence Lamp

Several benefits were obtained from the LED Fluorescence Lamp when compared to a conventional HBO lamp. First, the narrow wavelength, ≈ 25 nm according to Figure 6, outputted by the LED allows Bio-markers to fluoresce with a higher intensity than the broader wavelength mercury vapor lamp. Moreover, the time to switch on, and stabilize of 10-15 min from the mercury vapor lamp, was reduced to an instant output from the LED, thereby eliminating the disadvantages of the mechanical shutter from the original set-up. Additionally, the troubleshooting time of the system is faster, as if a problem with the LED diode arises, it can be addressed right away. The control module developed permits the regulation of the intensity yielded from the LED diode therefore neutral density filters are no longer needed, and a higher signal to noise ratio can be achieved. Secondly, the longer life-time with minimal decrease in optical power through hours of operation of the LED is, also, one of the main characteristics of the new LED fluorescence Lamp. Finally, the LED Fluorescence Lamp reduces lab cost operations, as, in average, the mercury bulbs would need to be replaced 3 times in the lifetime of one LED diode. Subsequently, reducing the amounts of mercury used and disposed of in the lab.

	Wavelength range	ON/OFF speed	Stabilization time	Intensity regulation	Spectrum	Optical Power	Mercury Disposal
HBO LAMP	300 nm - 850nm	ON- Milliseconds OFF- 30-minute cooldown	10 min - 15min	Not without filters.	Whole	Broad, decreases after 30 min.	Hazardous
LED LAMP	425 nm - 450nm	Instant	Milliseconds	Available with control module or filters.	Narrow	Specific, peaks when turned on	No hazardous disposal

Table 1- Comparison between traditional microscopy HBO Lamps and LED.

3.7 Discussion

Our results shown above, demonstrate the capability of the LED system developed to capture fluorescence at high resolution, high magnification systems. Observed fluorescence can be argued not to be as clear as with a conventional mercury vapor lamp, but we have found that the sensors used in the digital microscope cameras do not seem to be sensitive enough to the narrow spectrum produced by the LED fluorescence lamp. It is important to note that the manufacturer never states the capability of their sensors to capture fluorescence; yet with the right adjustment, quality results were obtained. Additionally, to the sensors, the lenses built within the Dino-Lite Digital Microscope cameras might be playing an important role in their sensitivity. In contrast to the Dino-Lite DMCs, the Microfire Optronics camera's higher quality sensors, and lenses prove to be suitable for further studies using the LED Fluorescence Lamp as excitation source of fluorescent tagged molecules .Equally important to the sensitivity of the recording cameras, the lenses built within the Zeiss Axiovert 25 CFL are believed to scatter some of the light emitted from the LED fluorescence Lamp before hitting the sample. Thus,limiting factors like budget, better camera sensors, and possibility of removing the lenses between the

sample and the improved LED fluorescence Lamp prevent the system to reach its full potential, but the results obtained demonstrate the capability of an LED system to provide a powerful light source for fluorescence microscopy studies Moreover, it opens the possibility of a future line of work in this field.

REFERENCES

1. Moore, W. (1972). Physical Chemistry. 4th ed. Englewood Cliffs, New Jersey: PRENTICE-HALL, INC, pp.794-797.

2. LV, Z., LU, J., WU, Y. and CHEN, L. (2010). Introduction to Theories of Several Super-resolution Fluorescence Microscopy Methods and Recent Advance in The Field*. *PROGRESS IN BIOCHEMISTRY AND BIOPHYSICS*, 2009(12), pp.1626-1634.

3. Hell, S. and Wichmann, J. (1994). Breaking the diffraction resolution limit by stimulated emission: stimulated-emission-depletion fluorescence microscopy. *Optics Letters*, 19(11), pp.780-782.

4. Huang, B., Bates, M. and Zhuang, X. (2019). Super resolution fluorescence microscopy. *Annual Review of Biochemistry*, 78:993-1016, pp.993-1016.

5. Hess, S., Girirajan, T. and Mason, M. (2006). Ultra-High Resolution Imaging by Fluorescence Photoactivation Localization Microscopy. *Biophysical Journal*, 91(11), pp.4258-4272.

6. van den Wildenberg, S., Prevo, B. and Peterman, E. (2018). A Brief Introduction to Single-Molecule Fluorescence Methods. *Methods of Molecular Biology*, 1665, pp.93-113.

7. Kenneth, S. and Michael, D. *Introduction to Fluorescence Microscopy* [online]. Nikon's MicroscopyU. Retrieved from https://www.microscopyu.com/techniques/fluorescence/introduction-to-fluorescence-microscopy [2019]

8. Abbe, E. (1882). The Relation of Aperture and Power in the Microscope (continued).*. *Journal of the Royal Microscopical Society, 2*(4), 460-473.

9. Beyond the diffraction limit [Editorial]. (2009, July 01). *Nature Photonics*, *3*

10. Silfies, J. S., Schwartz, S. A., & Davidson, M. J.. *The Diffraction Barrier in Optical Microscopy* [online] Nikon's MicroscopyU. Retrieved from

https://www.microscopyu.com/techniques/super-resolution/the-diffraction-barrier-in-optical-microscopy

11. Thorley, J. A., Pike, J., & Rappoport, J. Z. (2014). Fluorescence Microscopy Super-Resolution and Other Novel Techniques. In *Super-resolution Microscopy: A Comparison of Commercially Available Options* (1st ed., pp. 199-212). Academic Press.
12. Davidson, M. W. *Resolution* [online]. Nikon's MicroscopyU. Retrieved from https://www.microscopyu.com/microscopy-basics/resolution.

13. Pouyan, N. (2016). A Voyage to Beyond the Human Eye by Microscope, Leeuwenheoks Invention. *Open Access Library Journal, 03*(01), 1-9. Retrieved 2019.

14. Wollman, A. J., Nudd, R., Hedlund, E. G., & Leake, M. C. (2015). From Animaculum to single molecules: 300 years of the light microscope. *Open Biology, 5*(4), 150019-150019. Retrieved 2019.

15. Museum of Microscopy. (2019, November 13). Janssen's Microscope. Retrieved 2019, from https://micro.magnet.fsu.edu/primer/museum/janssen.html

16. Masters, B. R. (2008). History of the Optical Microscope in Cell Biology and Medicine. *Encyclopedia of Life Sciences,* 1-8. Retrieved 2019.

17. Singer C. (1914). Notes on the Early History of Microscopy. *Proceedings of the Royal Society of Medicine*, *7*(Sect Hist Med), 247-79.

18. Wimmer, W. (2017). Carl Zeiss, Ernst Abbe, and Advances in the Light Microscope. *Microscopy Today,25*(4), 50-57. Retrieved 2019.

19. Pluta, M. (1988). Phase Contrast Microscopy. In *Advanced Light Microscopy* (Vol. 2, pp. 1-11). Elsevier.

20. Nobel Media. (1964). Fritz Zernike- Biographical. In *Nobel Lectures* (Physics 1942-1962). Amsterdam: Elsevier.

21. Zernike, F. (1938). The concept of degree of coherence and its application to optical problems. *Physica, 5*(8), 785-795. Retrieved 2019.

22. Murphy, D. B., Oldfield, R., Schwartz, S., & Davidson, M. W. (2019). *Introduction to Phase Contrast Microscopy* [online]. Nikon's MicroscopyU. Retrieved 2019.

23. Graef, M. D. (n.d.). Phase contrast microscopy. Introduction to Conventional Transmission Electron Microscopy, 585-660.

24. Mann, C. J., Yu, L., Lo, C., & Kim, M. K. (2005). High-resolution quantitative phase-contrast microscopy by digital holography. *Optics Express, 13*(22), 8693-8698.

25. Barone-Nugent, E. D., Barty, A., & Nugent, K. A. (2002). Quantitative phase-amplitude microscopy I: Optical microscopy. *Journal of Microscopy, 206*(3), 194-203. Retrieved 2019.

26. Smith, F. H. (1955). Microscopic Interferometry. *Research, 8*, 385-395. Retrieved 2019.

27. Ruzin, S. (1999). Differentian Interference Contrast. In *Plant Microtechnique and Microscopy*. New York: Oxford University Press.

28. Nomarski Differential Interference Contrast Microscopy. (2004). *Encyclopedic Dictionary of Genetics, Genomics and Proteomics*. Retrieved 2019.

29. Murphy, D. (2001). Differential interference contrast (DIC) microscopy and modulation contrast microscopy. In *Fundamentals of Light Microscopy and Digital Imaging* (pp. 153-168). New York: Wiley-Liss.

30. Rost, F., & Oldfield, R. (2000). Differential interference-contrast (DIC) microscopy. In *Photography with a Microscope* (pp. 136-140). Cambridge, UK: Cambridge University Press.

31. Foster, B. (1997). Nomarski/DIC (Differential interference contrast). In *Optimizing Light Microscopy for Biological and Clinical Laboratories* (pp. 89-92). Dubuque, Iowa: Kendall/Hunt Publishing Company.

32. Pluta, M. (1994). Nomarski's DIC microscopy: A review. In *Phase Contrast and Differential Interference Contrast Imaging Techniques and Applications, SPIE Proceedings 1846* (pp. 10-25). International Society for Optical Engineering.

33. Milestones in light microscopy. (2009). *Nature Cell Biology, 11*(10), 1165-1165

34. Köhler, A., & Rohr, M. J. (1905). Photomicrography with ultra-violet light. *JR Microsc. Soc*, *25*, 513.

35. Heimstädt, O. (1911) Das Fluoreszenzmikroskop. Z. Wiss. Mikrosk. 28, 330–337

36. Freund, H. (1969). The role of Max Haitinger in the development of fluorescence microscopy. *Mikroskopie, 25*, 73-77. Retrieved 2019.

37. Haitinger, M. (1932). Methoden der Fluoreszenzanalyse. *Mikrochemie, 11*(1), 429-464. Retrieved 2019.

38. Ellinger, P., & Hirt, A. (1929). Mikroskopische Beobachtungen an lebenden Organen mit Demonstrationen (Intravitalmikroskopie). *Archiv Für Experimentelle Pathologie Und Pharmakologie, 147*(1-3), 63-63. Retrieved 2019.

39. Prashar, A., & Khan, F. (2013). Potential use of live fluorescence staining technique in surgery. *Clinical and Experimental Medical Sciences,* 291-298. Retrieved 2019.

40. Ploem, J. S. (1967). The use of a vertical illuminator with interchangeable dichroic mirrors for fluorescence microscopy with incidental light. *Z Wiss Mikrosk, 68*, 129-142. Retrieved 2019.

41. Elliott, D. J. (1995). Ultraviolet Light. *Ultraviolet Laser Technology and Applications,* 1-32. Retrieved 2019.

42. Mercury Vapor Lamp. (1913). *Journal of the Franklin Institute, 176*(3). Retrieved 2019.

43. Thompson, F. (1993). Ultraviolet Light. In *Encyclopedia of Food Science, Food Technology and Nutrition.* (2nd ed., pp. 5885-5890). London, UK: Elsevier.

44. Davidson, M. W. (n.d.). Education in Microscopy and Digital Imaging. Retrieved 2019.

45. Round, H. J. (1991). A Note on Carborundum. *Semiconductor Devices: Pioneering Papers,* 879-879. Retrieved 2019.

46. Lossev, O. (1928). CII.Luminous carborundum detector and detection effect and oscillations with crystals. *The London, Edinburgh, and Dublin Philosophical Magazine and Journal of Science,6*(39), 1024-1044. Retrieved 2019.

47. Destriau, G. (1937). Étude analytique des conditions d'excitation des phénomènes d'électro-photoluminescence. *Journal De Chimie Physique, 34*, 462-471. Retrieved 2019.

48. Lehovec, K., Accardo, C. A., & Jamgochian, E. (1951). Injected Light Emission of Silicon Carbide Crystals. *Physical Review, 83*(3), 603-607. Retrieved 2019.

49. Carr, W. N., & Pittman, G. E. (1963). ONE-WATT GaAs p-n JUNCTION INFRARED SOURCE. *Applied Physics Letters, 3*(10), 173-175. Retrieved 2019.

50. Hoerni, J. (1955). *U.S. Patent No. US3025589A*. Washington, DC: U.S. Patent and Trademark Office.

51. U.S. Department of Energy. (2008). Comparing LEDs to Traditional Light Sources. Retrieved 2019.

52. Electronic Design. (2013). Next-Generation GaN-on-Si White LEDs Suppress Costs. Retrieved 2019.

53. Worthey, J. (2006). How white light works. *LRO Lighting Research Symposium: Light and Color.* Retrieved 2019.

54. Roberts, S. (2009). Avoiding thermal runaway when driving multiple LED strings. *LEDs Magazine. Technology and Applications of Light Emitting Diodes.* Retrieved 2019.

55. BROADCOM. Avago Technologies. (2017). [Data Sheet — HLMP-1301, T-1 (3 mm) Diffused LED Lamps]. Raw data. Retrieved 2019.

56. Nichia Corporation. (2010, November). *High Power Point Source White Led NVSx219AWe rolled out a better idea* [Press release]. Retrieved 2019.

57. U.S. Department of Energy. (2008). Lifetime of White LEDs. Retrieved 2019.

58. Hohman, B., & Carl Zeiss Microimaging USA. (2018). LED Light Sources: A Major Advance in Fluorescence Microscopy [Editorial]. *Microscopy and Analysis*. John Wiley & Sons Ltd. Retrieved 2019.

59. Whoriskey, G. (2017). LEDs in Microscopy: An Emerging Research Tool. *Photonics Media.* Retrieved 2019.

60. Valeur, B. (2012). Introduction. In *Molecular Fluorescence: Principles and Applications* (2nd ed., pp. 3-19). Wiley-VCH Verlag GmbH & KGaA.

61. Valeur, B., & Berberan-Santos, M. N. (2011). A Brief History of Fluorescence and Phosphorescence before the Emergence of Quantum Theory. *Journal of Chemical Education,88*(6), 731-738. Retrieved 2019.

62. Fluorescence Foundation. (2018, December). *A Short History of Fluorescence*. Lecture presented at Principles of Fluorescence Techniques in Madrid, Spain.

63. Herschel, W. (1843). AFormula, No. 1. On a Case of Superficial Colour Presented by a Homogeneous Liquid internally Colourless. *Proceedings of the Royal Society of London,5*(0), 547-547. Retrieved 2019.

64. Herschel, W. (1845). AFormula, No. 2. On a Case of Superficial Colour Presented by a Homogeneous Liquid internally Colourless. *Proceedings of the Royal Society of London,5*(0), 147-153. Retrieved 2019.

65. Stokes, G. G. (1852). On the Change of Refrangibility of Light. *Philosophical Transactions of the Royal Society of London,142*, 1-17. Retrieved 2019.

66. Valeur, B. (2009). Molecular Fluorescence. In *Encyclopedia of Applied Spectroscopy.* (pp. 489-531). Weinheim: WILEY-VCH Verlag GmbH & KGaA.

67. Valeur, B. (2012). Characteristics of fluorescence emission. In *Molecular Fluorescence: Principles and Applications* (2nd ed., pp. 34-71). Wiley-VCH Verlag GmbH & KGaA.

68. Dino-Lite Digital Microscopes, *Dino-Lite Digital Microscopes.* Retrieved 2019.

69. Romo, J., Jr. (2016). Optical Method for Imaging and Video Recording Live Cultured Hela Cells at High Resolution, High Magnification. University of Texas Rio Grande Valley.

BIOGRAPHICAL SKETCH

Christian Yair Miranda Solis, 25, was born and raised in Mexico City, Mexico. He attended highschool at Instituto Tecnologico y de Estudios Superiores de Monterrey, Campus Estado de Mexico, where he graduated with a Bilingual Diploma. At the age of 18, he moved to the Rio Grande Valley and earned a bachelor's degree in Engineering Physics with a concentration in BioEngineering in 2016, and a Master of Science in 2019 at The University of Texas Rio Grande Valley. Under the supervision of Dr. Yong Zhou, he was member of "CHONOS", a team of undergraduate engineering students that participated in the NASA's Space Grant Consortium Design Challenge; where the team was given the with task of developing and Intelligent Lightning Control System capable of meeting the specifications for its use in a space shuttle. Team "CHRONOS" was awarded "Best Design". Furthermore, he worked under the supervision of Dr. Ahmed Touhami in developing an electrically controlled hydrogel capable of exhibiting exoskeleton characteristics. He graduated in the fall of 2016. In the spring of 2017, Dr. Juan Guevara Jr., and Dr. Natalia V. Guevara took him under their wing for his graduate studies. Christian worked as a research assistant in The Biophysics Research Laboratory participating in projects of sequence project analysis, and improvement of novel high-resolution, high-magnification microscopy techniques. It was under the mentorship of both, Dr. Juan, and Dr. Natalia, where he would not only receive training as a scientist but find advice and care to continue his personal growth. He considers both of them to be his second parents.

I can be reached at christianyairmirandasolis@gmail.com